Direct Measurements of Reynolds Stresses and Turbulence in the Bottom Boundary Layer

Joseph Katz
Department of Mechanical Engineering
The Johns Hopkins University
Baltimore, MD 21218
katz@titan.me.jhu.edu
phone: 410-516-5470
fax 410-516-7254

Thomas R. Osborn
Department of Earth and Planetary Sciences
The Johns Hopkins University
Baltimore, MD 21218
osborn@jhu.edu
phone: 410-516-7519
Fax 410 516-7933

Award #N00014510215

LONG-TERM GOALS

a) Measure the Reynolds stresses, velocity profile, vorticity, dissipation, and turbulent spectra in the bottom boundary layer of the coastal ocean using particle imaging velocimetry (PIV). The validity of these direct stress measurements is independent of assumptions about the boundary layer structure, turbulent spectra and balance of production and dissipation.

b) Quantify the temporal variation of turbulent stresses in relation to the oceanographic parameters that represent the local environment, such as waves, currents, vertical density gradient, internal wave regime, and nature of the water-sediment interface. The conclusions will be used to determine the relative importance of different mechanisms which control the velocity profile and the turbulent parameters in the benthic boundary layer of the coastal ocean.

c) Quantify the spatial variation of the stress in different environments to determine the relationship between point measurements and spatial averages, that are necessary for numerical modeling of coastal currents.

OBJECTIVES

The objective of this project is to directly measure the flow structure and turbulence, including the Reynolds stress, in the bottom boundary layer of the coastal ocean using particle image velocimetry (PIV).

APPROACH

Particle image velocimetry (PIV) is capable of mapping two components of the instantaneous velocity distribution within an entire section of a flow field. Although the actual implementation and analysis methods vary (Adrian, 1991), they all consist of illuminating the fluid with a laser sheet while seeding

Report Documentation Page

Form Approved
OMB No. 0704-0188

1. REPORT DATE **1998**	2. REPORT TYPE	3. DATES COVERED **00-00-1998 to 00-00-1998**

4. TITLE AND SUBTITLE **Direct Measurements of Reynolds Stresses and Turbulence in the Bottom Boundary Layer**	5a. CONTRACT NUMBER 5b. GRANT NUMBER 5c. PROGRAM ELEMENT NUMBER
6. AUTHOR(S)	5d. PROJECT NUMBER 5e. TASK NUMBER 5f. WORK UNIT NUMBER
7. PERFORMING ORGANIZATION NAME(S) AND ADDRESS(ES) **Johns Hopkins University,Department of Mechanical Engineering,Baltimore,MD,21218**	8. PERFORMING ORGANIZATION REPORT NUMBER
9. SPONSORING/MONITORING AGENCY NAME(S) AND ADDRESS(ES)	10. SPONSOR/MONITOR'S ACRONYM(S) 11. SPONSOR/MONITOR'S REPORT NUMBER(S)

12. DISTRIBUTION/AVAILABILITY STATEMENT
Approved for public release; distribution unlimited

13. SUPPLEMENTARY NOTES
See also ADM002252.

14. ABSTRACT

15. SUBJECT TERMS

16. SECURITY CLASSIFICATION OF:			17. LIMITATION OF ABSTRACT	18. NUMBER OF PAGES	19a. NAME OF RESPONSIBLE PERSON
a. REPORT **unclassified**	b. ABSTRACT **unclassified**	c. THIS PAGE **unclassified**	**Same as Report (SAR)**	**6**	

Standard Form 298 (Rev. 8-98)
Prescribed by ANSI Std Z39-18

the water with microscopic tracer particles. In oceanic applications the natural seeding, as available data and our own experience indicate, is generally sufficient. If the laser is pulsed more than once while recording a single (or two) image(s), each particle leaves multiple traces on the same (or successive) recording medium (media). The most popular approach to data analysis consists of dividing the image into a large number of small windows and computing the mean displacement of all the particles within each window. Typically, the analysis is based on computing the auto-correlation function of the intensity distribution within the selected window. In some applications, where spatial resolution is critical, the velocity is determined from the displacement of individual particles and the technique is referred to as particle tracking.

Unlike other instruments used for measuring the velocity distribution in the ocean, PIV provides an instantaneous two dimensional velocity distribution over the entire sample area. A sequence of measurements provides a time series of the spatial distribution, not just a time series of velocity at a single point. With such data available it is possible to obtain an overview of entire flow structures, and compute the vorticity distribution, rates of strain, turbulent stresses, turbulent spectra, spatial and temporal correlations, energy dissipation, etc. Since some of these variables require computations of velocity gradients, in time and in space, the error levels in velocity measurements should not exceed 1%.

WORK COMPLETED

Schematic descriptions of the mechanical hardware, optics, image acquisition and control systems of the bottom boundary layer system, that has already been deployed, are presented in Figure 1. For this system the sample area is 20x20 cm^2 and images are recorded using a 1024x1024 pixel digital camera that has a maximum image acquisition rate of 15 image-pairs per second, with essentially unlimited in-pair delay. The camera lens is equipped with a remote focusing system. The camera output is fed to a PC based image acquisition and processing system that has 2 processors, maximum acquisition rate of 100 MHz, 272 Mbytes of RAM (sufficient for 136 image pairs) and a slower hard disk. Data enhancement and velocity computation are performed directly on the processors. With 64x64 pixel windows and 50% overlap between windows, each 1Kx1K image provides an array of 29x29 velocity vectors.

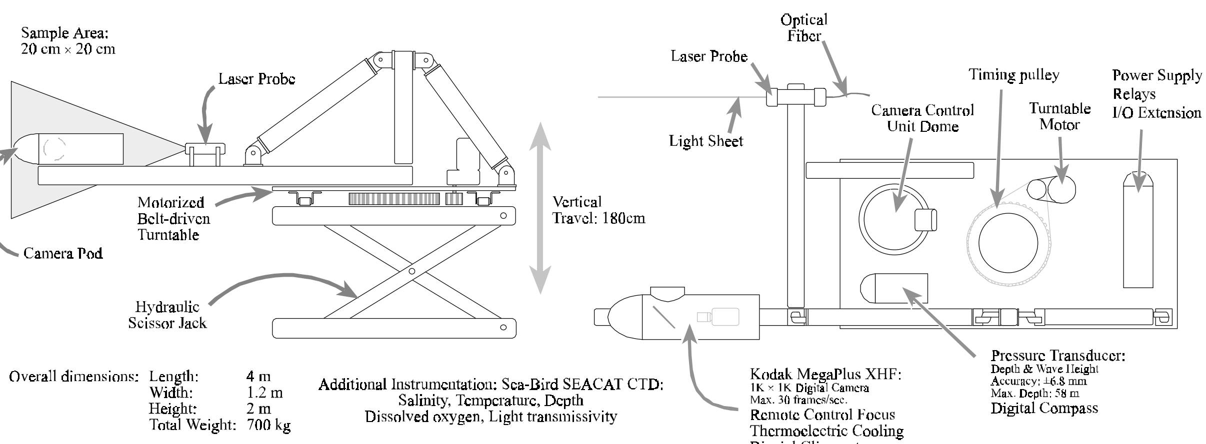

FIGURE 1: The submersible platform for bottom boundary layer measurements

To provide the required energy for extended periods we use an optical fiber to transmit the light from a surface mounted laser to the measurement area. We opted to use a high power pulsed laser, which presents difficulties in delivering high energies through a fiber. Based on the available literature a pulse duration of ~2 μs is needed for transmitting more than 100 mJ/pulse (the required level) through the fiber. The selected laser is a dual-head, flashlamp-pumped dye laser whose maximum output is 350 mJ/pulse at 595 nm, using Rhodamine 590 dye, at a maximum repetition rate of 2x15 Hz. Different wavelengths can be obtained using other dyes. The two beams are coupled into a single 400 μm diameter fiber. This core size is a compromise between a large core for better power handling and a small core for reducing the output beam divergence. The fiber terminates in a submerged probe which houses the optics for conditioning and expanding the beam to a sheet. The output achieved without difficulty is 126 mJ/pulse with a transmission efficiency of 91%. If damage occurs, it happens on the input face (located on the surface), and can be repaired by re-terminating the fiber in minutes.

In the setup for bottom boundary layer measurements the camera and laser sheet probes are mounted on modular optical rails which are connected to a support plate. The plate, along with the optics, can be rotated by a submerged motor. A hydraulic scissors-jack with a vertical travel of 1.8 m is used for varying the elevation of the system from the ocean floor up to an elevation of 2 m. The orientation and elevation of the sample area are remotely controlled. During deployment the platform carries a tilt meter and a digital compass for monitoring the orientation of the camera, a Sea Bird Sea-Cat CTD, an oxygen meter, a transmissometer and a Paroscientific Digiquartz pressure transducer for monitoring the surface waves. All the electronics for controlling the system and transmitting the data are also mounted on the same plate.

Expansion of the width of the sample area to 1 m: We are in the process of developing the next generation of oceanic PIV system, which is based on a pair of 2048X2048 pixel cameras. Each camera covers an (adjacent) area of 50x50 cm^2, thus providing an instantaneous velocity distribution in an area of 0.5 x 1.0 m^2 (the latter is the vertical direction). These custom-made cameras with digital image shifting can acquire up to four frames/s, which is sufficient for generating a “continuous” data base at speeds up to 2 m/s. This setup would provide data on a 1m wide strip of ocean flow. These cameras have been purchased and tested successfully in the laboratory. Their 12 bit data and 14 x 14 μm pixels have higher dynamic range and four times the sensitivity of the 1K x 1K camera. We are in the process of installing them in submersible enclosures and all the electronic interfaces have already been designed and tested. The laser has sufficient power for illuminating the enlarged sample area.

High Speed Image Acquisition System: A new image acquisition system that can support either the 1K x 1K camera or the new pair of 2K x 2K cameras has been constructed and already used during field tests in summer 1998. It can acquire data at rates of up to 30 MB/sec and feed it directly, through a wide-band SCSI adapter, to a bank of eight hard disks, each with a capacity of 9 GB (a total of 72 GB). This system can create a backup from disk to disk or to an integral tape drive while acquiring the data. It allows us to record 36,000 1K x 1K image pairs, i.e. we can acquire 1 Hz data continuously for 10 hours. At 15 image pairs/sec, we can acquire data for 40 minutes. With the 2Kx2K camera, acquiring 8 bit images, we can record 18,000 images. The disks that do not acquire data at a specific time can be unplugged and replaced during the experiment, which provides essentially unlimited capacity.

RESULTS

Measurements were made during early June, 1998 in a mud dumpsite covered with sand, 7 miles east of Highlands, NJ (40.423N, 73.857W). This data from the New York Bight was collected in 15m deep water, above a sandy bottom. Data for each elevation consists of 2 minutes of image pairs recorded at

1Hz and include the flow structure and Reynolds stress profiles within the inner layer. Figure 2 shows a sequence of 4 vector maps, where the mean velocity at each level has been subtracted from the measurements in order to show the turbulent fluctuations. We scanned the boundary layer starting from about 10 cm up to 1.4 m above the bottom. At each elevation we recorded a series of 20x20 cm image pairs, mostly at 1 Hz, but also at 15 Hz. The first set consisted of 2 minutes of 1 Hz data at six different elevations using the old acquisition system, i.e. 130 vector maps at each elevation. Then, using the new bank of hard disks, the second set consisted of 24 min of 1 Hz data at three elevations. Only the first set has been analyzed to-date (analysis is still in progress). In this data the amplitude of wave induced motion is only about 10% of the mean current (data not shown).

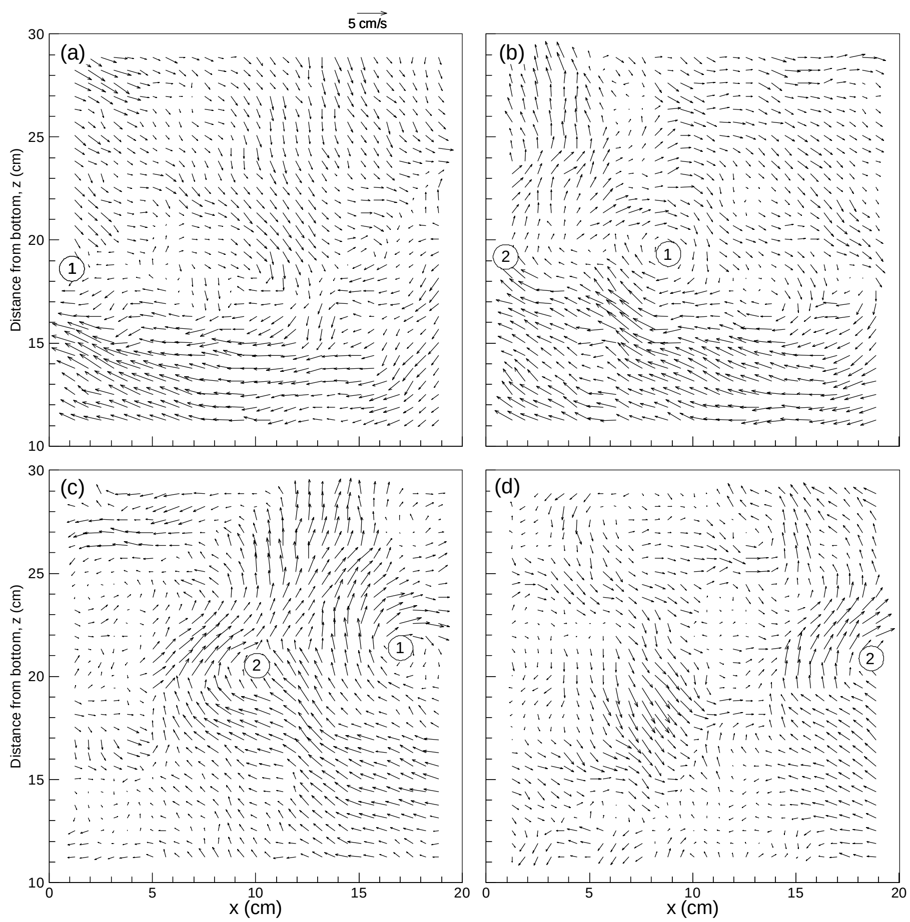

FIGURE 2: Sequence of velocity fluctuations vector maps measured in 14m deep water, at 1s intervals. u'(x,z)=u(x,z)-U(z), w'(x,z)=w(x,z)-W(z); u, w: Velocity components of a vector; U, W: Averages of u, w at constant z, over the entire data set. Note the structures designated "1" and "2" being convected across the sample area. Data from New York Bight, June 1998.

Sample distributions of velocity fluctuations, Reynolds stress and q^2 (where $q^2=3[u'^2+w'^2]/4$ is the estimated turbulent kinetic energy assuming that v'^2 is the average of $u'^2+w'^2$) are presented in Figure 3. Here u' is determined from the difference between the instantaneous and the average velocities at the same elevation for the entire set. To the best of our knowledge, this is the first well resolved data on the velocity and turbulence profile near the bottom. The results show that in the inner layer (z<25 cm) values of $-\overline{u'w'}$ are lower. Above this inner region the shear stress increases and remains fairly constant, whereas q^2 keeps increasing. *u'* maintains a level of about 12% of the maximum mean velocity (u_{max}=20.8 cm/s at the highest elevation) but its value relative to the local mean velocity increases rapidly near the bottom, where *u(z)* decreases to a third of u_{max}. *w'* decreases near the bottom and its level is significantly lower than *u'*. Thus, the turbulence is never isotropic and near the bottom is highly non-isotropic. For example, at an elevation of 15cm above the bottom, |u'|/U=33%, |w'|/U=12% and -u'w'/U^2=0.8%. Again, the data clearly indicates that 2 min averages are insufficient since *u(z)* varies with time, a problem that will be remedied with the available longer data set. An estimate of the external potential flow pressure gradient can also be computed from the vertical profile of U/W, and it indicates the existence of large scale phenomena, well beyond the time scale of the 130 second measurements. These trends will be resolved by analyzing the longer data series collected with the upgraded data acquisition system.

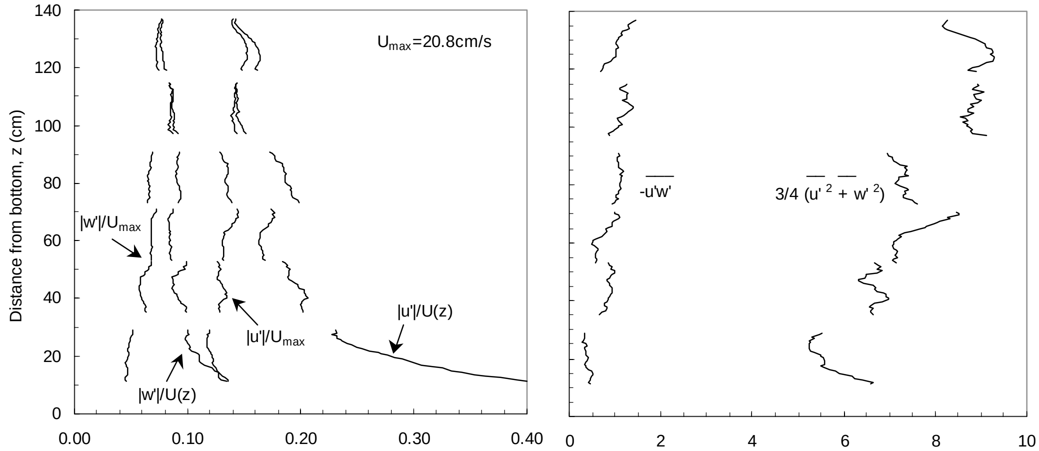

FIGURE 3: (a) Vertical profiles of RMS velocity fluctuations; (b) Vertical profiles of Reynolds stress and estimate for the turbulent kinetic energy, assuming v'=0.5(u'+w'). U_{max} is the largest value of U(z); Averages of u'^2, w'^2, u'w' are calculated at constant z, over the entire data set.

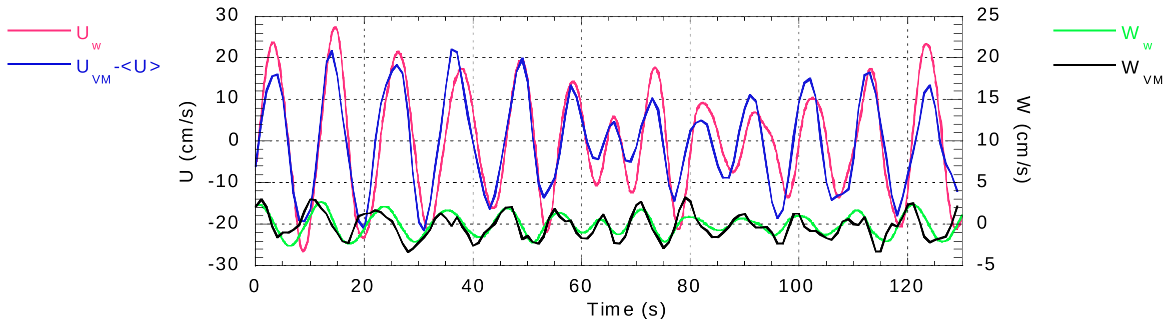

FIGURE 4: Time series of velocities computed from the pressure transducer data and linear wave theory (U_W, W_W), and average velocities measured with the PIV system. Subscript VM represents the average of the 841 vectors in an instantaneous vector map, <U> is the mean horizontal velocity for the entire data set.

Measurements were also performed 1.5 m above the ocean bottom, off Cape May, NJ, in October 1997. This data set consists of 130 vector maps, recorded at 1 Hz, each containing 29x29 vectors. The averaged velocity varies, and changes direction, due to surface waves with a period of about 10 sec. The data shows evidence of a beat with a period of about 7 wave periods. There is also a mean horizontal current of ~11.5 cm/s. The quarter-wave phase lag between the horizontal and vertical velocity components is characteristic of motion due to shallow water waves as confirmed by the comparison with linear wave theory shown in Figure 4.